

# Insight into the role of $\text{Li}_2\text{S}_2$ in Li-S battery: first-principles study

Guochun Yang<sup>a,b,\*</sup>, Shaoqing Shi<sup>a</sup>, Jinghai Yang<sup>c,\*</sup> and Yanming Ma<sup>b,\*</sup>

<sup>a</sup> Faculty of Chemistry, Northeast Normal University, Changchun 130024, China.

<sup>b</sup> State Key Laboratory of Superhard Materials, Jilin University, Changchun 130012, China.

<sup>c</sup> Institute of Condensed State Physics, Jilin Normal University, Siping 136000, P. R. China.

Index	page
1. Computational details .....	1
2. Bader and Mulliken atomic charge of $\text{Li}_2\text{S}_2$ and $\text{Li}_2\text{S}$ .....	2
3. Comparison of main structural parameters between our structure (a) and Zaghbi's structure (b) .....	3
4. The phonon frequencies and their infrared and Raman activity of $\text{Li}_2\text{S}_2$ .....	4
5. The phonon frequencies and their infrared and Raman activity of $\text{Li}_2\text{S}$ .....	5
6. References .....	6

## Computational details

Our structural prediction approach is based on a global minimization of free energy surfaces merging *ab initio* total-energy calculations through CALYPSO (Crystal structure AnaLYsis by Particle Swarm Optimization) methodology as implemented in its same-name CALYPSO code.<sup>1,2</sup> The structures of stoichiometry  $\text{Li}_m\text{S}_n$  ( $m = 1-4$ ,  $n = 1-4$ ) were searched with simulation cell sizes of 1–4 formula units (f.u.) at 1 GPa. In the first step, random structures with certain symmetry are constructed in which the atomic coordinates are generated by the crystallographic symmetry operations. Local optimizations using VASP code,<sup>3</sup> were done with the conjugate gradients method and were stopped when the enthalpy changes became smaller than  $1 \times 10^{-5}$  eV per cell. After processing the first generation structures, 60% of them with lower enthalpies are selected to produce the next generation structures by PSO. 40% of the structures in the new generation are randomly generated. A structure fingerprinting technique of bond characterization matrix is applied to the generated structures, so that identical structures are strictly forbidden. These procedures significantly enhance the diversity of the structures, which is crucial for the efficiency of the global search of structures. For most of the cases, the structure searching simulation for each calculation was stopped after we generated 1000 ~ 1200 structures (e.g., about 20 ~ 30 generations).

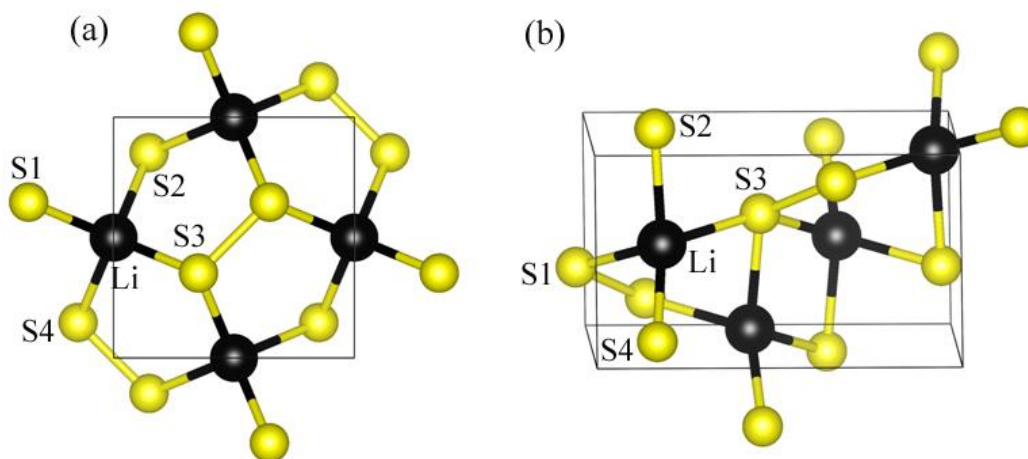
To further analyze the structures with higher accuracy, we select a number of structures with lower enthalpies and perform structural optimization using density functional theory within the generalized gradient approximation<sup>4</sup> as implemented in the VASP code. The cut-off energy for the expansion of wavefunctions into plane waves is set to 700 eV in all calculations, and the Monkhorst–Pack  $k$ -mesh with a maximum spacing of  $0.02 \text{ \AA}^{-1}$  was individually adjusted in reciprocal space with respect to the size of each computational cell. This usually gives total energy well converged within  $\sim 1 \text{ meV/atom}$ . The electron-ion interaction was described by means of projector augmented wave with  $s^1p^0$  and  $s^2p^4$  electrons as valence for Li and S atoms, respectively.

The density functional theory with the Perdew-Burke-Ernzerh (PBE) generalized

gradient approximation was employed in the phonon calculation as implemented in the QUANTUM-ESPRESSO package.<sup>5</sup> The Troullier–Martins normcon pseudopotentials were generated with valence atomic configurations of  $1s^2 2p^1$  and  $3s^2 3p^4$  for Li and S, respectively. The electronic wave functions and the electron density were expanded by the plane-wave basis sets with a cut-off energy of 70 Ry.  $14 \times 14 \times 12$  Monkhorst–Pack grids in the Brillouin zone were adopted. The choices of the above computational parameters ensured that the convergence of the phonon frequencies were within 0.08 THz.

**Table S1.** (a) Bader atomic charge and (b) Mulliken atomic charges (e) of  $\text{Li}_2\text{S}_2$ .

$\text{Li}_2\text{S}_2$	Bader <sup>a</sup>	Mulliken <sup>b</sup>
Li	0.87	0.84
Li	0.87	0.84
Li	0.87	0.84
Li	0.87	0.84
S	-0.87	-0.84
S	-0.87	-0.84
S	-0.87	-0.84
S	-0.87	-0.84



Our structure (a)				
Lattice parameters	Bond length (Å)		Bond angle ( ° )	
$a = b = 5.07$	S1-Li	2.47	$\angle(\text{S1-Li-S2})$	112.5
$c = 6.11$	S2-Li	2.47	$\angle(\text{S2-Li-S3})$	112.5
$\alpha = \beta = \gamma = 90.0$	S3-Li	2.47	$\angle(\text{S3-Li-S4})$	112.5
	S4-Li	2.47	$\angle(\text{S4-Li-S1})$	112.5
Zaghib's structure (b)				
Lattice parameters	Bond length (Å)		Bond angle ( ° )	
$a = 4.38; b = 4.68$	S1-Li	2.50	$\angle(\text{S1-Li-S2})$	109.9
$c = 7.47$	S2-Li	2.46	$\angle(\text{S2-Li-S3})$	88.15
$\alpha = \beta = 90.0$	S3-Li	2.49	$\angle(\text{S3-Li-S4})$	123.07
$\gamma = 109.7$	S4-Li	2.43	$\angle(\text{S4-Li-S1})$	102.61

**Figure S1.** Comparison of main structural parameters between our structure (a) and Zaghib's structure (b)

**Table S2.** The zone-center phonon modes, frequencies ( $\text{cm}^{-1}$ ), Infrared and Raman activities of  $\text{Li}_2\text{S}_2$ , and the experimental value of discharge product (Ref. 6).

Mode	Calculation	Experiment	Raman	Infrared
$E_u$	42.5			I
$A_{2u}$	53.8			I
$E_u$	135.9			I
$E_g$	138.6		R	
<b><math>B_{1g}</math></b>	<b>168.5</b>	<b>174</b>	<b>R</b>	
$B_{1u}$	172.7			
$A_{2g}$	220.7			
$E_g$	302.6		R	
$E_u$	330.2			I
$A_{1u}$	338.2			
$E_g$	355.7		R	
$E_u$	355.7			I
$A_{2u}$	356.1			I
$B_{1g}$	414.8		R	
$B_{2g}$	450.8		R	
$A_{1g}$	484.8		R	
<b><math>B_{2g}</math></b>	<b>499.9</b>	<b>514</b>	<b>R</b>	

**Table S3.** The zone-center phonon modes, frequencies ( $\text{cm}^{-1}$ ), Infrared and Raman activities, and experimental Raman frequencies ( $\text{cm}^{-1}$ ) (Ref. 7) of  $\text{Li}_2\text{S}$ .

Mode	Calculation	Experiment	Raman	Infrared
$T_{1u}$	-62.9			I
$T_{2u}$	191.8			
$T_{1u}$	192.8			I
$A_{2u}$	227.8			
$E_u$	227.8			
$T_{1g}$	237.8			
$T_{2g}$	237.8		R	
$T_{1u}$	240			I
$T_{1u}$	300.2			I
<b><math>T_{2g}</math></b>	<b>360.1</b>	<b>372</b>	<b>R</b>	
$T_{2u}$	367.4			
$T_{1u}$	368.6			I
$A_{1g}$	485.5		R	
$E_g$	487.6		R	

## Reference:

1. Wang, Y.; Lv, J.; Zhu, L.; Ma, Y. *Phys. Rev. B* **2010**, *82*, 094116.
2. Wang, Y.; Lv, J.; Zhu, L.; Ma, Y. *Comput. Phys. Commun.* **2012**, *183*, 2063.
3. Kresse, G.; Furthmuller, J. *Phys. Rev. B* **1996**, *54*, 11169.
4. Perdew, J. P.; Chevary, J. A.; Vosko, S. H.; Jackson, K. A.; Pederson, M. R.; Singh, D. J.; Fiolhais, C. *Phys. Rev. B* **1992**, *46*, 6671.
5. Giannozzi, P.; et al. *J. Phys.: Condens. Matter.* **2009**, *21*, 395502.
6. Diao, Yan.; Xie, K.; Xiong, S.; Hong, X. J. *Electrochem. Soc.* **2012**, *159*, A1816.
7. Seh, Z. W.; Wang, H.; Hsu, P-C.; Zhang, Q.; Li, W.; Zheng, G.; Yoo, H.; Cui, Y. *Energy. Environ. Sci.*, **2014**, *7*, 672.